A&A 571, A70 (2014)
DOI: 10.1051/0004-6361/201424288

Astronomy & Astrophysics

Revised age for CM Draconis and WD 1633+572

Toward a resolution of model-observation radius discrepancies

Gregory A. Feiden[1] and Brian Chaboyer[2]

[1] Department of Physics and Astronomy, Uppsala University, Box 516, 751 20 Uppsala, Sweden
e-mail: gregory.a.feiden@gmail.com
[2] Department of Physics and Astronomy, Dartmouth College, 6127 Wilder Laboratory, Hanover, NH 03755, USA

Received 27 March 2014 / Accepted 16 September 2014

ABSTRACT

We report an age revision for the low-mass detached eclipsing binary CM Draconis and its common proper motion companion, WD 1633+572. An age of 8.5 ± 3.5 Gyr is found by combining an age estimate for the lifetime of WD 1633+572 and an estimate from galactic space motions. The revised age is greater than a factor of two older than previous estimates. Our results provide consistency between the white dwarf age and the system's galactic kinematics, which reveal the system is a highly probable member of the galactic thick disk. We find the probability that CM Draconis and WD 1633+572 are members of the thick disk is 8500 times greater than the probability that they are members of the thin disk and 170 times greater than the probability they are halo interlopers. If CM Draconis is a member of the thick disk, it is likely enriched in α-elements compared to iron by at least 0.2 dex relative to the Sun. This leads to the possibility that previous studies under-estimate the [Fe/H] value, suggesting the system has a near-solar [Fe/H]. Implications for the long-standing discrepancies between the radii of CM Draconis and predictions from stellar evolution theory are discussed. We conclude that CM Draconis is only inflated by about 2% compared to stellar evolution predictions.

Key words. binaries: eclipsing – stars: evolution – stars: low-mass – stars: magnetic field – stars: individual: CM Draconis – stars: individual: WD 1633+572

1. Introduction

CM Draconis (also GJ 630.1 AC; hereafter CM Dra) is of fundamental importance for understanding low-mass stellar structure and evolution. CM Dra is a detached double-lined eclipsing binary (DEB) consisting of two mid-M-dwarf stars (Lacy 1977) whose masses and radii are known with high precision. The primary has a mass $M_A = 0.23102 \pm 0.00089\ M_\odot$ with a radius $R_A = 0.2534 \pm 0.0019\ R_\odot$ and the secondary has a mass $M_B = 0.21409 \pm 0.00083\ M_\odot$ with $R_B = 0.2398 \pm 0.0018\ R_\odot$ (Metcalfe et al. 1996; Morales et al. 2009; Torres et al. 2010). Both stars in CM Dra therefore have a mass below the nominal boundary where theory predicts stars to be fully convective throughout their interior ($M \sim 0.35\ M_\odot$; Limber 1958; Chabrier & Baraffe 1997).

The precision with which the fundamental properties of CM Dra are known allows for direct verification of predictions from stellar evolution theory. One of most basic predictions of the theory is the stellar mass-radius relationship. Below the fully convective boundary, predictions from stellar evolution models are largely insensitive to physical ingredients as the interiors are undergoing near-adiabatic convection. Variations of model predictions are typically at the 1% level, if provided with stringent constraints on the stellar metallicity and age. This caveat has typically been the limiting factor in rigorous tests of stellar evolution models, particularly for low-mass M-dwarfs (e.g., Young & Arnett 2005; Feiden & Chaboyer 2012a; Torres 2013). CM Dra is one of only two fully convective systems for which strong constraints can be placed on the these properties. Recent metallicity estimates converge toward a value of [Fe/H] = −0.3 ± 0.1 dex (Rojas-Ayala et al. 2012; Terrien et al. 2012a; Kuznetsov et al. 2012) and an age of 4 ± 1 Gyr has been estimated from a white dwarf (WD) common proper motion companion, WD 1633+572 (Morales et al. 2009).

At the given age and metallicity of CM Dra, stellar models are unable to accurately reproduce the observed radii (Feiden & Chaboyer 2014; MacDonald & Mullan 2014). Models predict radii that are 6.0% and 6.5% too small for the primary and secondary, respectively. The commonly cited explanation for the discrepancies is the presence of strong magnetic fields and/or magnetic activity (i.e., spots). These mechanisms inhibit convective energy transport causing the stars to inflate as they attempt to maintain a constant energy flux through the surface (Mullan & MacDonald 2001; Chabrier et al. 2007; MacDonald & Mullan 2012)[1]. Spots may also bias radius determinations from light curve data toward larger radii if present in an appropriate configuration, namely spots clustered near the poles (Windmiller et al. 2010; Morales et al. 2010). However, we recently argued that, while magnetic fields may be able to cause such effects, the required internal magnetic field strengths are on the order of 1–50 MG and are likely too strong to be stably supported within these stars (Feiden & Chaboyer 2014), a conclusion also reached by Chabrier et al. (2007). Additionally, we argued that star spot properties needed to reconcile models and observations are not

[1] We note that while spots are the physical manifestation of the suppression of convection locally on the stellar photosphere, they are often considered separately from magneto-convection (Mullan & MacDonald 2001; Chabrier et al. 2007) in 1D stellar evolution models.

yet supported by empirical evidence and that other avenues to reconcile models should therefore be explored.

Model assessments are predicated on the age and metallicity of CM Dra being correct and thus model discrepancies representing real departures of theory from observations. It has long been postulated that CM Dra is an old, Population II object (e.g., Lacy 1977; Chabrier & Baraffe 1995), but the WD age contradicts that assumption suggesting, instead, that the star is a Population I object. Here, we report a revision to the age of CM Dra based on modeling its common proper motion companion, WD 1633+572, that is supported by its galactic space motions. Sect. 2 contains the derivation of the revised age, followed in Sect. 3 by arguments that the age and galactic kinematics suggest the system may have a near-solar metallicity. We then synthesize the metallicity and age results in Sect. 4 and assess the impact of our results on the noted radius inflation in Sect. 5. Finally, we provide a brief discussion of additional implications for the study in Sect. 6.

2. Age estimate

2.1. White dwarf age

WD 1633+572 is a DQ WD showing shifted C_2 Swan bands as well as C_2H absorption (Giammichele et al. 2012). These peculiarities are thought to be characteristic of a He dominated atmosphere which has recently dredged up carbon from the bottom of the thin convective envelope (Hansen 2004). An age estimate for WD 1633+572, and therefore CM Dra, was previously provided by Morales et al. (2009) who found the system to be 4.1 ± 0.8 Gyr old. Their result relied on combing an estimate of the WD cooling age with an approximate lifetime of the WD progenitor star. Cooling tracks predicted a WD cooling age of 2.84 ± 0.37 Gyr for a 0.63 ± 0.04 $M_\odot$ WD (Bergeron et al. 2001). Stellar evolution models provided a progenitor star lifetime of about 1.3 Gyr assuming the progenitor star had a mass of 2.1 ± 0.4 $M_\odot$ (Catalán et al. 2008).

However, recent advances in WD atmosphere and cooling models lead to a downward revision of the mass for WD 1633+572. The new estimate is $M_{\rm wd} = 0.57 \pm 0.04\ M_\odot$ (Giammichele et al. 2012). Decreasing the WD mass will increase the radius and decrease the WD cooling age, as a result. Giammichele et al. (2012) predict the cooling age of WD 1633+572 is 2.62 Gyr, slightly younger than before. An independent analysis of WD 1633+572 confirms the mass and age estimate (M. Salaris, priv. comm.; Salaris et al. 2010). Cooling tracks from Salaris et al. (2010) yield a WD age of 3.4 ± 0.6 Gyr, consistent with previous estimates, within the error bars. This latter analysis allowed for phase separation during crystallization, which leads to an increase in the cooling age, and can account for about half of the difference between the Salaris et al. (2010) and Giammichele et al. (2012) estimates.

Although the WD cooling age is not dramatically affected by updated cooling tracks, the lower mass estimate suggests that revision of the progenitor mass – and age – is needed. There are multiple initial–final mass relations (IFMRs), each which predict different progenitor masses: $M_{\rm p} = 1.5 \pm 0.5\ M_\odot$ (Catalán et al. 2008), $M_{\rm p} = 1.3 \pm 0.4\ M_\odot$ (Kalirai et al. 2009), and $M_{\rm p} = 1.6 \pm 0.9\ M_\odot$ (Zhao et al. 2012). Variation may be expected given that these studies sample different parameter regimes for WDs using different methods. The aforementioned relations all include WDs with masses around 0.57 $M_\odot$, but it should be noted that none contain WDs with a similar mass and $T_{\rm eff}$ as WD 1633+572. Instead of selecting a single IFMR upon which to base the progenitor mass estimate, we take an uncertainty weighted average of those values listed above and find $M_{\rm p} = 1.4 \pm 0.3\ M_\odot$. This revised mass represents a significant reduction in the progenitor mass compared to Morales et al. (2009) and translates into a significant age increase of the progenitor star lifetime.

Using standard Dartmouth stellar evolution models (Dotter et al. 2008; Feiden & Chaboyer 2014), we evolve models at 1.1 $M_\odot$, 1.4 $M_\odot$, and 1.7 $M_\odot$ with a metallicity of −0.3 dex. Progenitor ages are taken to be the age of the model at the tip of the red giant branch (tRGB), as subsequent phases of evolution do not contribute appreciably to the overall progenitor age. From these three models, we estimate the age of the progenitor star to be $3.1^{+3.8}_{-1.3}$ Gyr, where the errors represent the errors on the mean value. The combined WD cooling age plus progenitor age for WD 1633+572 is then $6.5^{+4.4}_{-1.9}$ Gyr. However, this age is subject to further revision due to possible abundance revisions for CM Dra presented in Sect. 3.

2.2. Kinematic age

Disagreement has been previously noted between the age of WD 1633+572 and the age inferred from the system's kinematics (Morales et al. 2009). The WD age is characteristic of the system belonging to the galactic thin disk population, while the system's high proper motion suggests a kinematically older age with a possible Population II origin.

CM Dra has proper motions of $\mu_\alpha = -1109$ mas yr^{-1} and $\mu_\delta = 1203$ mas yr^{-1} and WD 1633+572 has commensurate values of $\mu_\alpha = -1106$ mas yr^{-1} and $\mu_\delta = 1206$ mas yr^{-1} (Lépine & Shara 2005). Parallaxes of both objects were obtained in the US Naval Observatory parallax program (Harrington & Dahn 1980). CM Dra has a parallax of $\pi = 68 \pm 4$ mas and WD 1633+572 has a parallax of $\pi = 61 \pm 6$ mas, indicating the two systems are approximately equidistant from the Sun. The parallax of CM Dra has been revised to $\pi = 69.2 \pm 2.5$ mas by the Yale Trigonometric Parallax program (van Altena et al. 1995), but the Yale program did not provide a revision for WD 1633+572. Still, the parallaxes between the two objects are consistent within the errors.

There are strong disagreements in the literature between the measured radial velocities (RVs) of CM Dra and WD 1633+572. The absolute RV for CM Dra is a by-product of accurate RV monitoring over 10 years in order to measure the masses of the two stars (Metcalfe et al. 1996; Morales et al. 2009). These authors find $\gamma = -118.24 \pm 0.07$ km s^{-1}, although they admit that the uncertainty in this value is almost certainly larger. An independent study by Karataş et al. (2004) finds a value of $\gamma = -118.71$ km s^{-1}, confirming the RV measurement. However, the absolute RV for WD 1633+572 is quoted to be $\gamma = 3.4$ km s^{-1} (Silvestri et al. 2002; Sion et al. 2009, 2014). Such a difference in the RVs of CM Dra and WD 1633+572 precludes the notion that they share a common origin.

Investigation of this issue revealed that the quoted RV for WD 1633+572 was based on a single RV measurement of CM Dra (Silvestri et al. 2002). This was motivated by the fact that the two systems share a common high-proper motion and are, then, likely coeval. Therefore, the absolute RV of CM Dra could be safely projected onto WD 1633+572. However, it is likely that the authors did not realize that CM Dra was itself a tight M-dwarf binary. Relying on only a single spectrum of CM Dra likely produced an incorrect RV. Knowing that the absolute RV of WD 1633+572 was assumed by the authors to be

equal to that of CM Dra, it should be revised to $\gamma = -118$ km s^{-1}, rescuing the assumption that the systems share a common origin.

We find galactic space velocities of $(U, V, W) = (105 \pm 4, -120 \pm 1, -36 \pm 2)$ km s^{-1} for CM Dra and $(U, V, W) = (119 \pm 9, -123 \pm 3, -31 \pm 4)$ km s^{-1} for WD 1633+572, where the uncertainties are based only on the uncertainty in the measured parallaxes. Note that the sign of the U velocity coordinate is with respect to galactic *anti*-center. Corrections for the local standard of rest were not applied.

While it is not possible to definitively associate any single star with a galactic population, it is possible to assign a relative probability that a star belongs to a given stellar population. Assignment of relative probabilities follows the procedure adopted by Bensby et al. (2005). They assume galactic space velocity distributions for the thin disk, thick disk, and stellar halo are Gaussian with resulting probabilities normalized to the observed fraction of stars in the solar neighborhood (see Appendix A of Bensby et al. 2005, 2014). Given their velocity dispersions and asymmetric drifts for the three kinematic populations, we find that CM Dra is about 8500 times more likely to be a member of the galactic thick disk than the galactic thin disk. Similarly, CM Dra is 170 times more likely to belong to the thick disk than the galactic halo. It therefore appears statistically unlikely that CM Dra is a member of the thin disk and is better suited as a member of the thick disk. Although it is not impossible to imagine a scenario whereby CM Dra is a highly perturbed thin disk star, we shall provide further evidence that the properties of CM Dra are consistent with a possible thick disk membership.

We note that Sion et al. (2014) claim that all local WDs within 25 pc are very likely members of the thin disk, including WD 1633+572. However, their membership claim is based on an erroneous RV measurement for CM Dra, which leads to *UVW* space velocities consistent with thin disk membership. With the correct RV value, it is very likely that WD 1633+572 is a local member of the thick disk population.

Assignment to the thick disk population has consequences for both the age and chemical composition of CM Dra. It is thought that the thick disk formed relatively early in the history of our Galaxy-about 11 Gyr ago-but star formation was truncated after ~1 to 2 Gyr had elapsed. This scenario is supported by the imprint of various stellar population on chemical enrichment history of thick disk stars (e.g., Bensby et al. 2007, 2014) and by age estimates some of the oldest WDs in globular clusters and the solar neighborhood, which are between 9 and 12 Gyr (Hansen et al. 2013; Salaris et al. 2010), for an average of about 10.5 ± 1.5 Gyr. There is also strong evidence suggesting that thick disk stars have a range of metallicities, from metal-poor up to solar values (Bensby et al. 2007). However, thick disk stars can be distinguished from thin disk stars by the fact that they appear enriched in α-elements (Bensby et al. 2010, 2014; Adibekyan et al. 2013). At [Fe/H] = −0.3 dex, thick disk stars are characterized by [α/Fe] ~ +0.2 dex to +0.4 dex. If CM Dra is a member of the thick disk population, we may infer that it is α-enhanced with an age of 10.5 ± 1.5 Gyr old.

3. Impact on metallicity determination

Assuming that CM Dra is a member of the galactic thick disk, and thus α-element enriched, has implications for M-dwarf metallicity determinations based on calibrations of near-infrared (NIR) equivalent widths (EWs) (e.g., Terrien et al. 2012b; Rojas-Ayala et al. 2012). These calibrations are performed on wide binaries in the solar neighborhood with an FG primary and an M-dwarf companion, where the metallicity of the FG primary is measured and projected onto the M-dwarf. Since the binaries are in the solar neighborhood, the calibration sample is biased toward thin disk stars with solar-like distributions of heavy elements. Increasing [α/Fe], particularly [O/Fe], increases the level of continuum suppression caused by H_2O molecules in the NIR at a given [Fe/H]. As a consequence, NIR atomic line depths will appear weaker with respect to a normalized pseudo-continuum than in the case of a solar-like metal distribution. Metallicity determinations based on EWs of NIR atomic lines are then expected to produce [Fe/H] values that are too low when applied to a star that is *unknowingly* α-enhanced compared to the Sun.

To test the influence of an enhanced [α/Fe] on the abundance determination of CM Dra, we applied the metallicity calibration of Terrien et al. (2012b) to a series of PHOENIX BT-SETTL synthetic spectra (Allard et al. 2012). The spectra had [Fe/H] = 0.0 with a Caffau et al. (2011) solar composition, $\log(g) = 5.0$, and ranged in $T_{\rm eff}$ from 3000 K to 3300 K. There were two sets of spectra with these parameters, one set with [α/Fe] = 0.0 and the other set with [α/Fe] = 0.2. Since the original EW calibration was performed using spectra with $R \sim 2000$, we degraded the synthetic spectra by convolving them with a Gaussian kernel. Examples of the resulting spectra at 3 200 K in the wavelength regions used for the Terrien et al. (2012b) metallicity determination are shown in Fig. 1. For reference, Fig. 1 also shows the same spectra degraded to $R \sim 40\,000$, where atomic features are more easily identified.

Applying the Terrien et al. (2012b) [Fe/H] calibration to each spectrum in the series, we find that α-enhanced spectra yield [Fe/H] values that are systematically lower by 0.1 dex−0.3 dex than spectra with a solar α-abundance. Results of this analysis are tabulated in Table 1. This difference is independent of the degraded spectral resolution and whether one uses the H- or K-band relation, but it is dependent on $T_{\rm eff}$. Differences increase with decreasing $T_{\rm eff}$. Temperature dependence is expected as H_2O absorption increases with decreasing $T_{\rm eff}$ at constant metallicity, a trend that is supported by empirical data (Rojas-Ayala et al. 2012). Therefore, increasing the relative abundance of H_2O will have a larger impact at cooler $T_{\rm eff}$, as was found in our analysis.

From Table 1, we see that the metallicity calibration does not successfully reproduce the [Fe/H] value of the synthetic spectra. This is likely a reflection of both uncertainties in synthetic model atmospheres and slight differences in continuum normalization. We stress that this is not a reflection of the intrinsic quality of the metallicity calibration. Rojas-Ayala et al. (2012) demonstrated that the K-band Na I doublet is weaker in BT-SETTL spectra than in empirical data. Additionally, they showed that BT-SETTL spectra possess weaker Ca I triplet lines in the relevant $T_{\rm eff}$ range. This suggests one would derive lower [Fe/H] values from synthetic spectra. However, at shorter wavelengths, Ca I features appear stronger in BT-SETTL spectra. Assuming that Ca I lines continue to appear stronger in the H-band, we would expect to find higher [Fe/H] values returned from the H-band calibration. These trends are consistent with offsets in the [Fe/H] determinations listed in Table 1 at solar [α/Fe]. Curiously, we note that the average abundance between the H- and K-band is accurate.

Although the absolute [Fe/H] determination is suspect when applied to synthetic spectra, these errors will be mitigated in a relative abundance study to assess the impact of α-enhancement. Additional errors may be present in the strength of Ca I features since Ca is an α-element, but there should be no relative impact on the strength of Na or K atomic features. Looking at

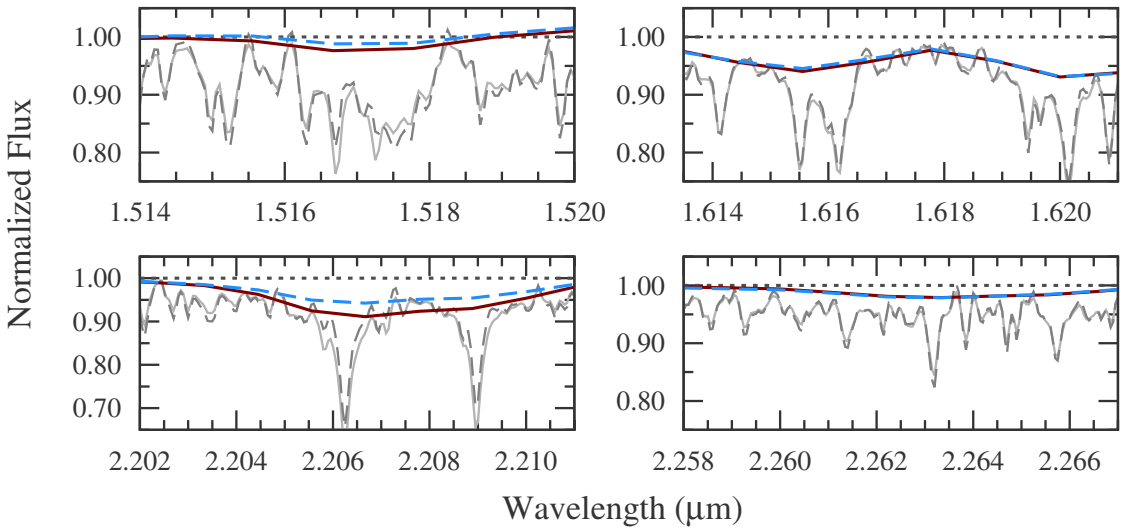

Fig. 1. Synthetic PHOENIX BT-SETTL stellar spectra in the four wavelength regions utilized in the Terrien et al. (2012b) NIR EW metallicity calibration. Spectra are shown for a star with $T_{\rm eff}$ = 3200 K, log(g) = 5.0, and [Fe/H] = 0.0 with [α/Fe] = 0.0 (maroon, solid lines) and +0.2 (light-blue, dashed lines). These have been degraded to an approximate spectral resolution $R \sim 2000$. For reference, the same spectra are shown with spectral resolution $R \sim 40\,000$.

Table 1. Metallicity determinations for PHOENIX BT-SETTL spectra calculated using a NIR EW calibration.

$T_{\rm eff}$	[α/Fe] = +0.0		[α/Fe] = +0.2			
(K)	[Fe/H]$_H$	[Fe/H]$_K$	[Fe/H]$_H$	[Fe/H]$_K$	Δ[Fe/H]$_H$	Δ[Fe/H]$_K$
3000	+0.19	−0.23	−0.10	−0.49	−0.29	−0.27
3100	+0.25	−0.24	+0.01	−0.48	−0.24	−0.24
3200	+0.31	−0.27	+0.13	−0.47	−0.18	−0.20
3300	+0.38	−0.27	+0.27	−0.44	−0.11	−0.17

the Δ[Fe/H] values in Table 1, one sees the differences between metallicity errors introduced by α-enhancement are consistent between H-band calibration results (equally dominated by the EW of Ca I and K I) and K-band calibration results (dominated by the Na doublet). Errors due to the additional abundance of Ca I do not appear to strongly affect the results.

We conclude that CM Dra may have an [Fe/H] about 0.2 dex higher than quoted by Terrien et al. (2012a), assuming a $T_{\rm eff} \approx$ 3200 K. This implies [Fe/H] = −0.1 ± 0.1 dex with [α/Fe] = 0.2 dex. Since CM Dra and WD 1633+572 are assumed to have a common origin, the progenitor of WD 1633+572 should be modeled with the same abundance. Increasing the overall metallicity of the progenitor will act to increase its lifetime and therefore increase the age of the system.

4. Final age

The association of CM Dra and WD 1633+572 with the galactic thick disk leads to a revision of the properties of the WD progenitor. Stellar models must be computed with [α/Fe] = +0.2 dex and assuming [Fe/H] = −0.1 dex. Computing models at the same progenitor masses as in Sect. 2 yields a progenitor age estimate of $3.8^{+4.8}_{-1.4}$ Gyr. WD 1633+572 then appears to have an age of $7.2^{+5.4}_{-2.0}$ Gyr. If we assume that the oldest age must correspond to the maximum age of the thick disk (about 12 Gyr), then the age may be written $7.2^{+4.8}_{-2.0}$, or 8.5 ± 3.5 Gyr if all ages in this range are equally likely a priori. This age is consistent with previous estimates, within the error bars, but represents nearly a factor of two increase in the mean value.

Furthermore, updates to WD atmosphere models, cooling models, and the IFMR lead to consistent age estimates between WD age-dating of WD 1633+572 and the association of CM Dra and WD 1633+572 with the galactic thick disk population via kinematics. The WD age is still highly uncertain (within 30%) due to uncertainty in the IFMR and thus an uncertainty in the progenitor star lifetime. However, considering the minimum age for a thick disk member is in the vicinity of 9 Gyr, the WD age provides good agreement. There exists the question of whether a 9−12 Gyr old thick disk object can be characterized by [Fe/H] = −0.1 while still showing signatures of α-enhancement. There is evidence that FGK stars with this abundance pattern exist (Bensby et al. 2007, 2010, 2014; Adibekyan et al. 2013), where the more metal-rich thick disk members are the product of subsequent star formation and enrichment episodes. Bensby et al. (2007) suggest that chemical enrichment of thick disk stars carried on until about 8 or 9 Gyr ago, which is largely consistent with the age derived for CM Dra and the finding that it possesses a significantly high metallicity for a thick disk star. We infer that a probable age for CM Dra is anywhere between 8 and 12 Gyr, given its likely association with the thick disk. For modeling purposes, we will avoid constraining the age further and adopt the formal age range of 8.5 ± 3.5 Gyr.

5. Implications for stellar evolution theory

Dartmouth stellar evolution models are used to assess the impact on both standard stellar models (Dotter et al. 2008; Feiden & Chaboyer 2014) and those that include magnetic field effects (Feiden & Chaboyer 2012b).

5.1. Standard stellar evolution models

Figure 2 provides a comparison between standard stellar evolution model predictions and the observed properties of CM Dra. After about 5 Gyr, evolutionary effects become noticeable and model radii increase over their zero-age-main-sequence value. At the former age of 4 Gyr, the model radii have not evolved significantly, compared to the zero-age-main-sequence values, and are about 6% discrepant with observations. However, at 7.2 Gyr, models of the primary shown in Fig. 2 have radii of 0.2450 $R_\odot$, 0.2467 $R_\odot$, and 0.2487 $R_\odot$ for [Fe/H] = −0.2, −0.1, and 0.0, respectively. These correspond to relative radius errors of 3.3%, 2.6%, and 1.9%, respectively, or deviations at the 4.4σ, 3.5σ, and 2.5σ level. Similarly, for the secondary, models have radii at 7.2 Gyr of 0.2306 $R_\odot$, 0.2322 $R_\odot$, and 0.2341 $R_\odot$ for the same metallicities, respectively. Discrepancies with the secondary are larger at 3.8%, 3.2%, and 2.4%, or 5.1σ, 4.2σ, and 3.2σ, respectively. Notably, while the radii are incorrectly predicted, the effective temperature ratio between the two models agrees with the observed value within the error bars. For [Fe/H] = −0.1 dex, $T_{\rm eff}$ = 3297 K and 3270 K for the primary and secondary, respectively, giving a temperature ratio equal to 0.9918, effectively consistent with the observed value of 0.996 ± 0.004 (Morales et al. 2009). While increasing the age and overall metal abundance of the stellar models helps to relieve the size of the radius discrepancies, significant (3σ) discrepancies remain.

If we instead assume that CM Dra is formally a member of the thick disk, and thus nominally between the age of 8 and 12 Gyr, the discrepancies between models and observations is further lessened. From Fig. 2, we find that a model of the primary has a radius R = 0.2493 $R_\odot$ for [Fe/H] = −0.1 dex at 10 Gyr yielding a relative radius error of 1.6% (2.2σ). A model of the secondary has a radius of 0.2339 $R_\odot$, which is 2.5% (3.3σ) discrepant with the observations. The temperature ratio remains equal to 0.9918, as above. One can further reduce the discrepancies by assuming an older age. Nevertheless, the models can not be completely reconciled with the observations for ages less than the age of the Universe.

5.2. Magnetic stellar evolution models

Stellar model mass tracks with magnetic fields are shown in Fig. 3. Two formulations of the influence of magnetic fields are shown: a rotational dynamo with a dipole radial magnetic field strength profile, and a constant-Λ turbulent dynamo (see Feiden & Chaboyer 2014, for details). In general, the turbulent dynamo formulation does not provide an adequate solution, whereas a rotational dynamo with a 5.0 kG surface magnetic field strength is able to provide agreement. In addition to matching the observed stellar radii, the rotational dynamo models are able to maintain agreement with the observed effective temperature ratio between the two components. Primary and secondary $T_{\rm eff}$s are reduced to 3032 K and 3015 K, respectively, for a ratio of 0.9944. As in Feiden & Chaboyer (2014), the interior magnetic field strength peaks at about 50 MG, making the magnetic field buoyantly unstable. However, by shifting the radial location of the peak interior magnetic field strength from $R = 0.15\,R_\star$ to $R = 0.50\,R_\star$, we are able to reduce the peak magnetic field strength from 50 MG to 50 kG, for the quoted 5.0 kG surface magnetic field strength, while still maintaining agreement between the models and observations between 7.2 and 12.0 Gyr. This revised value is more inline with expected magnetic fields strengths from 3D magnetohydrodynamic models (Chabrier & Küker 2006; Browning 2008).

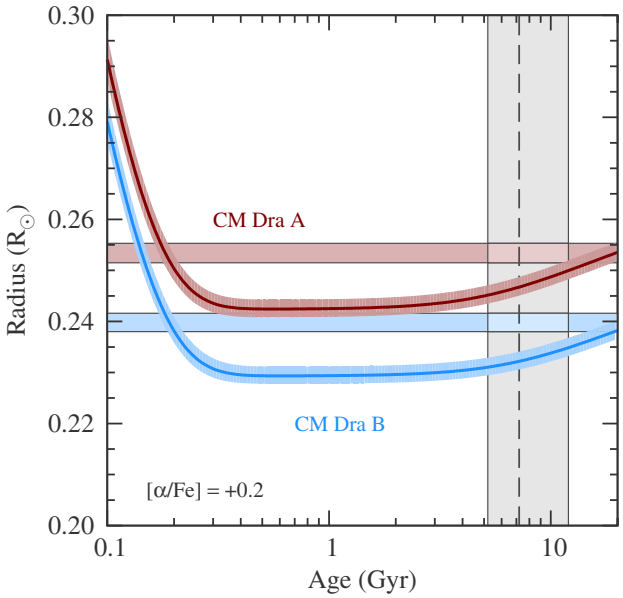

Fig. 2. Standard Dartmouth models computed at the precise masses of the CM Dra stars with [Fe/H] = −0.1 ± 0.1 dex with [α/Fe] = +0.2 dex. Solid lines show the evolution of models with [Fe/H] = −0.1 dex and the band surrounding those tracks show the predicted variation with metallicity. The lower bound of the uncertainty band corresponds to [Fe/H] = −0.2 dex, while the upper band corresponds to solar metallicity. For reference, the horizontal shaded regions mark the observed radius with 1σ uncertainties. The vertical stripe denotes the age constraint determined in Sect. 4, with a vertical dashed line marking an age of 7.2 Gyr.

Feiden & Chaboyer (2014) discussed that the surface magnetic field has little effect on the radius inflation in fully convective stars, particularly CM Dra. However, the reduction in the model-observation radius discrepancies from 6% to 3% means that the model does not need to develop a radiative core or shell through stabilization of convection. Surface effects appear more able to correct the discrepancies when they are reduced to a few percent. We note that a 5.0 kG average surface magnetic field is stronger, by about a factor of two, than the typical value of 3 kG observed on fully convective stars, again raising questions as to the validity of the magnetic models for these stars (e.g., Reiners 2012).

To reduce the surface magnetic field strength, we must instead compensate with larger interior magnetic fields. Thus, although the desired radius inflation is relatively small compared to previous studies, models still require a magnetic field strength of around 1 MG, which is at risk of being buoyantly unstable. This requirement is unavoidable in current 1D magneto-convection prescriptions that aim to stabilize the stellar interior against convection. A simple order of magnitude estimate illustrates this fact. Convection in fully convective stars is nearly-adiabatic, with $\nabla - \nabla_{\rm ad} \sim 10^{-6}$. Magneto-convection prescriptions used by MacDonald & Mullan (2012) and Feiden & Chaboyer (2012b) depend on $\nabla - \nabla_{\rm ad}$ being larger than some value ϵ, which is primarily set by the ratio of the magnetic pressure to the gas pressure. Therefore, convection will be suppressed when $\epsilon \sim 10^{-6}$. Gas pressure deep in the stellar interior is $\sim 10^{16}$ to 10^{17} dyne cm^{-2}, meaning the magnetic pressure must be $\sim 10^{10}$ to 10^{11} dyne cm^{-2}. This corresponds to a magnetic field strength of about 10^6 G. One way out of this requirement is through a turbulent dynamo, but as Fig. 3 shows, more advanced

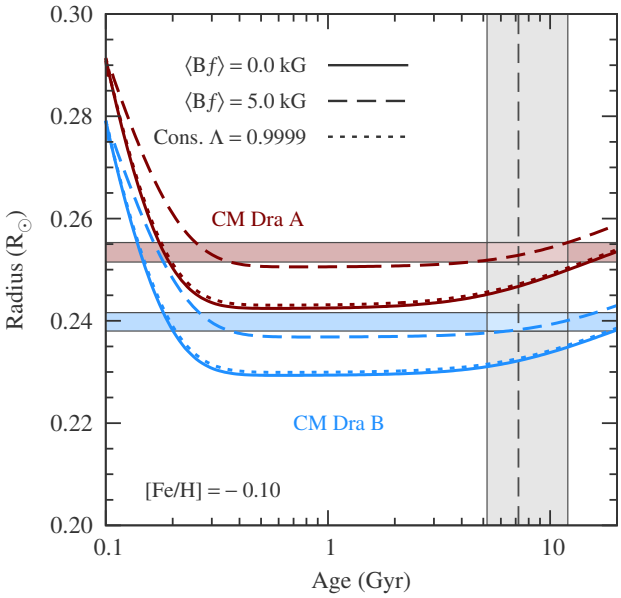

Fig. 3. Magnetic stellar evolution model tracks of the CM Dra stars. Models are computed at the precise masses of the CM Dra stars with [Fe/H] = −0.1 dex and [α/Fe] = +0.2 dex. Solid lines show the evolution of models with no magnetic field, for reference. Magnetic models with a "rotational dynamo" and dipole radial profile are shown as dashed lines while dotted lines are magnetic models computed with a constant-Λ radial profile with a "turbulent dynamo". Horizontal shaded regions mark the observed radius with 1σ uncertainties. The vertical stripe denotes the age constraint determined in Sect. 4.

techniques need to be explored if it is to impart significant structural changes.

5.3. Star spots

We can, instead, consider star spots to be the source of the observed inflation (Chabrier et al. 2007; Morales et al. 2010), due to both the biasing of radius measurements and actual structural changes inflicted on the stars. Taking both effects into account, 10% of the surface would need to be covered in completely dark spots. Assuming only a radius bias or only structural changes lead to 16% and 25% coverages, respectively. Since spots are not necessarily completely dark, but simply cooler than the surrounding photosphere, adopting a temperature contrast of 90% (Berdyugina 2005; Feiden & Chaboyer 2014) leads to equivalent surface coverages of 30%, 46%, and 64%, for the aforementioned cases, respectively. For radius biasing to occur, which has a more substantial influence than structural changes, spots are required to be located preferentially at the poles. In principle, spots can be detected by detailed modeling of spectral line profiles, with polar cap spots often providing clear signal of their presence (e.g., Berdyugina 2005). An observational search for polar cap spots on CM Dra is underway.

Assuming that a fraction of the stellar surface is covered in dark spots, one can also estimate the expected level of light curve modulation. Numerical experiments were carried out by Morales et al. (2010) to investigate this relationship. With 10% surface coverage, they found light curve modulation amplitude in the *R*-band was typically greater than 4%, with the exact number depending on the distribution of spots and the assumed spot sizes. CM Dra was observed to have a modulation amplitude in the *R*-band of 3% (Morales et al. 2009). It is therefore conceivable that the light curve modulation could be fit assuming a 10% coverage fraction. A more complete spot analysis exploring the entire parameter space would need to be performed, but is beyond the scope of this study. However, the key fact is that based on the work of Morales et al. (2010), the spots must be preferentially located at the poles.

6. Discussion

6.1. Orbital eccentricity

A rather curious feature of the CM Dra system is its mild orbital eccentricity (e = 0.05; Metcalfe et al. 1996; Morales et al. 2009). In its present configuration, the stars in CM Dra are expected to synchronize their rotation and circularize their orbit within roughly 0.3 Gyr (Zahn 1977). Thus, the presence of an elliptical orbit is rather perplexing. Though WD 1633+572 could cause perturbations to the orbit of CM Dra, at a projected distance of roughly 370 AU, the overall impact on the orbit over time is likely to be negligible owing to the short orbital period of CM Dra (Morales et al. 2009). It has therefore been proposed that CM Dra is host to a fourth body in the form of either a massive planet or low-mass brown dwarf (Deeg et al. 2008; Morales et al. 2009), though evidence for such a companion has yet to be firmly established.

Another suggested interpretation might be that CM Dra is in fact younger than it appears, not having time to circularize its orbit. However, we know that WD 1633+572 is at least 2.8 Gyr old, based on the cooling tracks alone and ignoring the progenitor lifetime. Circularization, it was mentioned, should occur for this system within roughly 0.3 Gyr. Though the tidal circularization calculation is only an order of magnitude estimate, it suggests that a younger age would not provide a sufficient explanation for the observed eccentricity, unless of course, WD 1633+572 and CM Dra do not have a common origin and are instead the product of a stellar encounter.

6.2. Mass-radius problem for low-mass stars

Revisions to the properties of CM Dra advanced in this paper are unable to provide a complete solution to the mass–radius discrepancies. However, the disagreements are significantly reduced from of order 6% to between 2% and 3%, further highlighting the need for accurate metallicities and reasonable age constraints if comparisons with stellar evolution models are to be meaningful (Young & Arnett 2005; Feiden & Chaboyer 2012a; Torres 2013). Additional uncertainties introduced by unknown He abundances complicate the matter (Valcarce et al. 2013). Increasing the He abundance of the stars in CM Dra to a value of Y = 0.35 (compared to Y = 0.28 in aforementioned models) can produce a 2% radius increase, and thus lead to agreement between observations and theory. Subpopulations of stars in a few globular clusters show evidence of having significantly enhanced helium abundances ($Y \sim 0.35$–0.40), as in NGC 2808 (Milone et al. 2012; Marino et al. 2014) and Omega Centauri (Bellini et al. 2010; Dupree et al. 2011; Dupree & Avrett 2013). Presently, there is no evidence for such helium enhancement among field stars in the halo or thick disk and models that can explain the multiple populations observed in globular clusters are not applicable to field stars. Thus, there is no observational evidence or theoretical arguments to support the idea that CM Dra may be significantly enhanced in helium. Furthermore, such a prediction is at risk of being observationally untestable.

Decreasing disagreements to the 2% level does raise the question, "How accurate can one expect stellar evolution models

to be?" The level of uncertainty in stellar models is often around 1%, given current microphysics, making 2% deviations potentially significant. The significance of the deviations are reinforced by the fact that no well characterized fully convective stars appear smaller than models, indicating a systematic offset. On the other hand, this also highlights the need for observers to mitigate systematics, especially those from spots that may be introducing errors on the order of 1 to 3% (Windmiller et al. 2010; Morales et al. 2010). Studies aimed at increasing the number of fully convective stars with empirically determined star spot maps would provide a valuable contribution.

6.3. Confirming α-enrichment

The hypothesis that CM Dra is a thick disk member requires confirmation. Evidence presented throughout this paper, we believe, lends strong support to the idea, but the evidence presented is circumstantial. Identifying spectral signatures of α-enhancement would provide the strongest evidence, as α-enhancement leads to the notion that the metallicity is near-solar. Investigations are ongoing to identify unambiguous signatures in optical and NIR spectra.

One further implication of CM Dra being α-enhanced is that it may possibly reconcile disagreements among various metallicity estimates, which are well-documented (see, e.g., Terrien et al. 2012a, and references therein). Molecular features in optical spectra leads to near-solar metallicities (Gizis 1997), as do NIR photometric colors (Leggett et al. 1998). However, line modeling of atomic features and CO bands in the NIR yield consistently lower metallicities around -0.6 to -1.0 dex (Viti et al. 1997, 2002; Kuznetsov et al. 2012), whereas NIR EW calibrations (Rojas-Ayala et al. 2012; Terrien et al. 2012a) and NIR photometric relations (Johnson & Apps 2009) yield more intermediate values, as discussed earlier. Synthetic spectra that are α-enhanced display molecular features in the optical that are similar to non-α-enhanced spectra, whereas in the NIR, additional continuum suppression can lead to weaker atomic features, as well as weaker CO features. The former would lead one to a more correct metallicity, while the latter occurrences would provide lower metallicities. It has been previously suggested that CM Dra is chemically peculiar (Viti et al. 1997, 2002), so perhaps this is the manifestation of α-enhancement. We are continuing to investigate this possibility.

Acknowledgements. The authors thank the anonymous referee for giving helpful comments and suggestions to improve the manuscript and M. Salaris for providing a cooling track analysis of the white dwarf. G.A.F. thanks B. Gustafsson, O. Kochukhov, E. Stempels, and T. Nordlander for stimulating discussion and helpful suggestions. The Dartmouth magnetic stellar evolution code was developed with support from the National Science Foundation (NSF) grant AST-0908345. This work made use of NASA's Astrophysics Data System (ADS) and the SIMBAD database, operated at CDS, Strasbourg, France.

References

Adibekyan, V. Z., Figueira, P., Santos, N. C., et al. 2013, A&A, 554, A44
Allard, F., Homeier, D., & Freytag, B. 2012, Roy. Soc. London Philos. Trans. Ser. A, 370, 2765
Bellini, A., Bedin, L. R., Piotto, G., Milone, A. P., Marino, A. F., & Villanova, S. 2010, AJ, 140, 631
Bensby, T., Feltzing, S., Lundström, I., & Ilyin, I. 2005, A&A, 433, 185
Bensby, T., Zenn, A. R., Oey, M. S., & Feltzing, S. 2007, ApJ, 663, L13
Bensby, T., Alves-Brito, A., Oey, M. S., Yong, D., & Meléndez, J. 2010, A&A, 516, L13
Bensby, T., Feltzing, S., & Oey, M. S. 2014, A&A, 562, A71
Berdyugina, S. V. 2005, Liv. Rev. Sol. Phys., 2, 8
Bergeron, P., Leggett, S. K., & Ruiz, M. T. 2001, ApJS, 133, 413
Browning, M. K. 2008, ApJ, 676, 1262
Caffau, E., Ludwig, H.-G., Steffen, M., Freytag, B., & Bonifacio, P. 2011, Sol. Phys., 268, 255
Catalán, S., Isern, J., García-Berro, E., & Ribas, I. 2008, MNRAS, 387, 1693
Chabrier, G., & Baraffe, I. 1995, ApJ, 451, L29
Chabrier, G., & Baraffe, I. 1997, A&A, 327, 1039
Chabrier, G., & Küker, M. 2006, A&A, 446, 1027
Chabrier, G., Gallardo, J., & Baraffe, I. 2007, A&A, 472, L17
Deeg, H. J., Ocaña, B., Kozhevnikov, V. P., et al. 2008, A&A, 480, 563
Dotter, A., Chaboyer, B., Jevremović, D., et al. 2008, ApJS, 178, 89
Dupree, A. K., & Avrett, E. H. 2013, ApJ, 773, L28
Dupree, A. K., Strader, J., & Smith, G. H. 2011, ApJ, 728, 155
Feiden, G. A., & Chaboyer, B. 2012a, ApJ, 757, 42
Feiden, G. A., & Chaboyer, B. 2012b, ApJ, 761, 30
Feiden, G. A., & Chaboyer, B. 2014, ApJ, 786, 53
Giammichele, N., Bergeron, P., & Dufour, P. 2012, ApJS, 199, 29
Gizis, J. E. 1997, AJ, 113, 806
Hansen, B. 2004, Phys. Rep., 399, 1
Hansen, B. M. S., Kalirai, J. S., Anderson, J., et al. 2013, Nature, 500, 51
Harrington, R. S., & Dahn, C. C. 1980, AJ, 85, 454
Johnson, J. A., & Apps, K. 2009, ApJ, 699, 933
Kalirai, J. S., Saul Davis, D., Richer, H. B., et al. 2009, ApJ, 705, 408
Karataş, Y., Bilir, S., Eker, Z., & Demircan, O. 2004, MNRAS, 349, 1069
Kuznetsov, M. K., Pavlenko, Y. V., Jones, H., & Pinfield, D. J. 2012, Adv. Astron. Space Phys., 2, 15
Lacy, C. H. 1977, ApJ, 218, 444
Leggett, S. K., Allard, F., & Hauschildt, P. H. 1998, ApJ, 509, 836
Lépine, S., & Shara, M. M. 2005, AJ, 129, 1483
Limber, D. N. 1958, ApJ, 127, 363
MacDonald, J., & Mullan, D. J. 2012, MNRAS, 421, 3084
MacDonald, J., & Mullan, D. J. 2014, ApJ, 787, 70
Marino, A. F., Milone, A. P., Przybilla, N., et al. 2014, MNRAS, 437, 1609
Metcalfe, T. S., Mathieu, R. D., Latham, D. W., & Torres, G. 1996, ApJ, 456, 356
Milone, A. P., Piotto, G., Bedin, L. R., et al. 2012, A&A, 537, A77
Morales, J. C., Ribas, I., Jordi, C. et al. 2009, ApJ, 691, 1400
Morales, J. C., Gallardo, J. J., Ribas, I., et al. 2010, ApJ, 718, 502
Mullan, D. J., & MacDonald, J. 2001, ApJ, 559, 353
Reiners, A. 2012, Liv. Rev. Sol. Phys., 8, 1
Rojas-Ayala, B., Covey, K. R., Muirhead, P. S., & Lloyd, J. P. 2012, ApJ, 748, 93
Salaris, M., Cassisi, S., Pietrinferni, A., Kowalski, P. M., & Isern, J. 2010, ApJ, 716, 1241
Silvestri, N. M., Oswalt, T. D., & Hawley, S. L. 2002, AJ, 124, 1118
Sion, E. M., Holberg, J. B., Oswalt, T. D., et al. 2009, AJ, 138, 1681
Sion, E. M., Holberg, J. B., Oswalt, T. D., et al. 2014, AJ, 147, 129
Terrien, R. C., Fleming, S. W., Mahadevan, S., et al. 2012a, ApJ, 760, L9
Terrien, R. C., Mahadevan, S., Bender, C. F., et al. 2012b, ApJ, 747, L38
Torres, G. 2013, Astron. Nachr., 334, 4
Torres, G., Andersen, J., & Giménez, A. 2010, A&ARv, 18, 67
Valcarce, A. A. R., Catelan, M., & De Medeiros, J. R. 2013, A&A, 553, A62
van Altena, W. F., Lee, J. T., & Hoffleit, E. D. 1995, The general catalogue of trigonometric [stellar] parallaxes (New Haven: Yale University Observatory)
Viti, S., Jones, H. R. A., Schweitzer, A., et al. 1997, MNRAS, 291, 780
Viti, S., Jones, H., Maxted, P., & Tennyson, J. 2002, MNRAS, 329, 290
Windmiller, G., Orosz, J. A., & Etzel, P. B. 2010, ApJ, 712, 1003
Young, P. A., & Arnett, D. 2005, ApJ, 618, 908
Zahn, J.-P. 1977, A&A, 57, 383
Zhao, J. K., Oswalt, T. D., Willson, L. A., Wang, Q., & Zhao, G. 2012, ApJ, 746, 144